Histol Histopathol (2023) 38: 797-810

Histology and Histopathology
From Cell Biology to Tissue Engineering

ORIGINAL ARTICLE Open Access

Circ_0007385 promotes the proliferation and inhibits the apoptosis of non-small cell lung cancer cells via miR-337-3p-dependent regulation of LMO3

Mingchao Wei*, Rongjiang Yin*, Li Qu and Jian Tang

Department of Thoracic Surgery, Yantai Affiliated Hospital of Binzhou Medical University, PR China

*Equal contribution

Summary. Background. This study intended to analyze the expression characteristic, functions and underlying mechanism of circular RNA_0007385 (circ_0007385) in non-small cell lung cancer (NSCLC).

Methods and Results. RNA and protein expression was examined by real-time quantitative polymerase chain reaction (RT-qPCR) and Western blot assay. Cell counting kit 8 (CCK8) assay, colony formation assay, 5-Ethynyl-2'-deoxyuridine (EdU) assay and flow cytometry were applied to analyze cell proliferation ability. Flow cytometry was also conducted to assess cell apoptosis. Dual-luciferase reporter assay and RNA immunoprecipitation (RIP) assay were performed to verify the predicted target relationships. Xenograft tumor model was utilized to analyze the function of circ_0007385 *in vivo*, and immunohistochemistry (IHC) assay was used to analyze protein expression in xenograft tumor tissues. Circ_0007385 expression was notably enhanced in NSCLC tissues and cell lines. Circ_0007385 facilitated the proliferation but suppressed the apoptosis of NSCLC cells. Circ_0007385 acted as a sponge for microRNA-337-3p (miR-337-3p), and circ_0007385 overexpression-mediated effects were largely overturned by the overexpression of miR-337-3p in NSCLC cells. MiR-337-3p interacted with the 3' untranslated region (3'UTR) of LIM-only protein 3 (LMO3). Circ_0007385 up-regulated LMO3 level by absorbing miR-337-3p in NSCLC cells. LMO3 overexpression largely reversed miR-337-3p overexpression-induced influences in NSCLC cells. Circ_0007385 knockdown significantly restrained the growth of xenograft tumors *in vivo*.

Conclusion. Circ_0007385 promoted the proliferation ability and inhibited the apoptosis of NSCLC cells by binding to miR-337-3p to induce LMO3 expression.

Key words: Non-small cell lung cancer, circ_0007385, miR-337-3p, LMO3

Introduction

Non-small cell lung cancer (NSCLC) is a common pulmonary malignancy (Molina et al., 2008). Although a considerable amount of studies have been performed in NSCLC treatment, the overall survival of NSCLC patients is still dismal, which is accompanied by a high recurrence rate (Toloza et al., 2003). Therefore, identifying novel bio-markers in NSCLC monitoring and prognosis is necessary for NSCLC treatment.

Circular RNAs (circRNAs) are newly-identified endogenous circular RNA molecules (Greene et al., 2017). Circ_0007385 was identified to exert an oncogenic role in NSCLC by previous articles (Jiang et al., 2018; Ye et al., 2020; Lin et al., 2020). For instance, Jiang et al. found that circ_0007385 facilitated the proliferation capacity and motility in NSCLC cells (Jiang et al., 2018). We further investigated the working mechanism of circ_0007385 in NSCLC development.

CircRNAs serve as molecular sponges for microRNAs (miRNAs) to modulate cellular physiological and pathological processes (Panda, 2018). For instance, circ_0082182 level was enhanced in colorectal cancer, and it contributed to colorectal cancer progression by absorbing miR-411 and miR-1205 (Liu et al., 2021). Based on bioinformatics analysis, miR-337-3p possessed the complementary sites with circ_0007385. MiR-337-3p blocked NSCLC progression as verified by former studies (Du et al., 2012; Li et al., 2019). For instance, miR-337-3p accumulation elevated the chemo-sensitivity of NSCLC cells (Du et al., 2012). In this study, the functional association of circ_0007385 and miR-337-3p in regulating phenotypes in NSCLC cells was explored.

Corresponding Author: Jian Tang, Jinbu Street, Muping District, Yantai City, Shandong Province, 264100, PR China. e-mail: ajhhbnm@163.com

www.hh.um.es. DOI: 10.14670/HH-18-553

LIM-only protein 3 (LMO3) belongs to the LMO protein family, and it plays vital modulatory roles in cell proliferation and differentiation during embryonic development (Dawid et al., 1998). In NSCLC, LMO3 was identified to exert its carcinogenic role to promote NSCLC progression, and it was reversely modulated by miR-382 (Chen et al., 2019) and miR-630 (Song et al., 2015). LMO3 possessed potential binding sites with miR-337-3p via bioinformatics analysis. We investigated the function of miR-337-3p/LMO3 axis in NSCLC cells.

We aimed to assess expression pattern and biological significance of circ_0007385 in NSCLC. In addition, the intermolecular binding relations among circ_0007385, miR-337-3p and LMO3 were uncovered.

Materials and methods

Tumor tissue samples

Forty-two NSCLC patients, who underwent surgical resection without chemo- or radiotherapy, were enrolled at Yantai Affiliated Hospital of Binzhou Medical University. Pairs of NSCLC specimens and adjacent normal lung tissue specimens (2 cm from the lesion) were collected from these patients. Written informed consents were signed by all cases. Human tissue specimens were utilized upon the permission of the Ethics Committee of Yantai Affiliated Hospital of Binzhou Medical University.

Cell lines

Normal control cell line (16HBE) and a panel of NSCLC cell lines (SK-MES-1, NCI-H2342, Calu-3, HCC827, NCI-H1975, NCI-H1299 and A-549) were acquired from Shanghai Academy of Sciences (Shanghai, China). Roswell Park Memorial Institute-1640 (RPMI-1640) medium (Gibco, Carlsbad, CA, USA) and Dulbecco's modified Eagle's medium (DMEM) medium (Gibco) were utilized for cultivation of NSCLC cell lines and 16HBE cell line. The media was added with 10% fetal bovine serum (FBS; Gibco) and 1% antibiotic mixture (Sangon Biotech, Shanghai, China) for cell culture.

RNA expression determination via real-time quantitative polymerase chain reaction (RT-qPCR)

Template DNA was acquired via commercial RevertAid First-Strand cDNA Synthesis kit (for circRNA and messenger RNA (mRNA); Thermo Fisher Scientific, Foster City, CA, USA) and MicroRNA Reverse Transcription Kit (for miRNA; Applied Biosystems, Foster City, CA, USA). Thermal cycling amplification reaction was performed using template DNA, primers (Table 1) and Amplification Mix (Thermo Fisher Scientific). Glyceraldehyde-phosphate dehydrogenase (GAPDH) and U6 acted as controls. $2^{-\Delta\Delta Ct}$ method was adopted to evaluate gene abundance (Livak and Schmittgen, 2001).

Determination of subcellular localization

The ratio of circ_0007385 in cytoplasmic fraction and nuclear fraction was assessed using the PARIS kit (Invitrogen, Carlsbad, CA, USA). GAPDH and U6 served as the references of cytoplasm and nucleus, respectively.

RNase R digestion

Exonuclease RNase R was acquired from Epicentre Technologies (Madison, WI, USA). RNAs were digested with 3 U/μg RNase R for 40 min. RT-qPCR was adopted to analyze abundance of circ_0007385 and mediator of cell motility 1(MEMO1) mRNA.

Cell transfection

Overexpression plasmid of circ_0007385 (circ_0007385), empty vector (Vector), small interfering (si)RNAs targeting circ_0007385 (si-circ_0007385#1 and si-circ_0007385#2), siRNA control (si-con), short hairpin RNA targeting circ_0007385 (sh-circ_0007385), shRNA control (sh-con), specific mimics of miR-337-3p (miR-337-3p), specific inhibitor of miR-337-3p (in-miR-337-3p) and their negative controls (miR-NC and in-miR-NC), LMO3 overexpression plasmid (LMO3), empty pcDNA vector (pcDNA), siRNA targeting LMO3 (si-LMO3) and siRNA NC (si-NC) were purchased from Sangon Biotech and Genepharma (Shanghai, China). For cell transfection, plasmids or RNAs were introduced into NSCLC cells via commercial Lipofectamine 3000 reagent (Invitrogen).

Proliferation determination via cell counting kit 8 (CCK8) assay

At indicated time points, a total of 10 μL CCK8

Table 1. Primers in RT-qPCR.

gene		primer (5'-3')
circ_0007385	forward	GTTTGAACGCATGTCTCTGC
	reverse	GCAGCACAAGACCCACAGTA
MEMO1	forward	ACGTACTGTGGGTCTTGTGC
	reverse	ACTGTGTTCATCTTCATCTG
miR-337-3p	forward	TCGGCAGGCTCCTATATGATGC
	reverse	CTCAACTGGTGTCGTGGA
miR-485-3p	forward	TCGGCAGGGTCATACACGGCTC
	reverse	CTCAACTGGTGTCGTGGA
LMO3	forward	GAGACTATCTGAGGCTCTTT
	reverse	TCATGTTATTCTTTAGGAAA
U6	forward	CTCGCTTCGGCAGCACA
	reverse	AACGCTTCACGAATTTGCGT
GAPDH	forward	ATGTTGCAACCGGGAAGGAA
	reverse	AGGAAAAGCATCACCCGGAG

reagent (Dojindo, Tokyo, Japan) was pipetted for 2h incubation with NSCLC cells. Absorbance in each well was determined using microplate reader (Bio-Rad, Hercules, CA, USA).

Colony formation assay

Transfected NSCLC cells were seeded onto 12-well plates at low density of 150 cells/well. Cells were cultured for 14 days at 37°C incubator to form colonies. Colonies were immobilized using 4% paraformaldehyde stationary liquid (EpiZyme, Shanghai, China) and stained via 0.1% commercial crystal violet liquor (EpiZyme). Colony number was manually counted.

5-Ethynyl-2'-deoxyuridine (EdU) assay

DNA synthesis was assessed through analyzing the incorporation of EdU to measure cell proliferation ability via KeyFluor488 EdU Kit (keyGEN Biotech, Jiangsu, China). NSCLC cells were incubated with 20 μM EdU reagent, and 4, 6-diamino-2-phenylindole dye liquor (DAPI; Sigma, St. Louis, MO, USA) was utilized to stain the nucleus. The fluorescence intensities were detected via the fluorescence microscope (Olympus, Tokyo, Japan) at 100×.

Flow cytometry for cell cycle analysis and apoptosis analysis

Muse Cell Cycle Assay Kit (Millipore, Billerica, MA, USA) was utilized to analyze cell cycle progression. After immobilizing using 70% ethanol (Sangon Biotech), DNA content in cells was stained using propidium iodide (PI; Sigma). Cell samples were loaded onto a flow cytometer (BD Biosciences, San Jose, CA, USA).

Commercial Annexin V and Dead Cell kit (Millipore) to test cell apoptosis. Phosphatidylserine and DNA in cells were marked via fluorescein isothiocyanate (FITC)-conjugated Annexin V and PI. Cell samples were loaded onto a flow cytometer (BD Biosciences), and cell

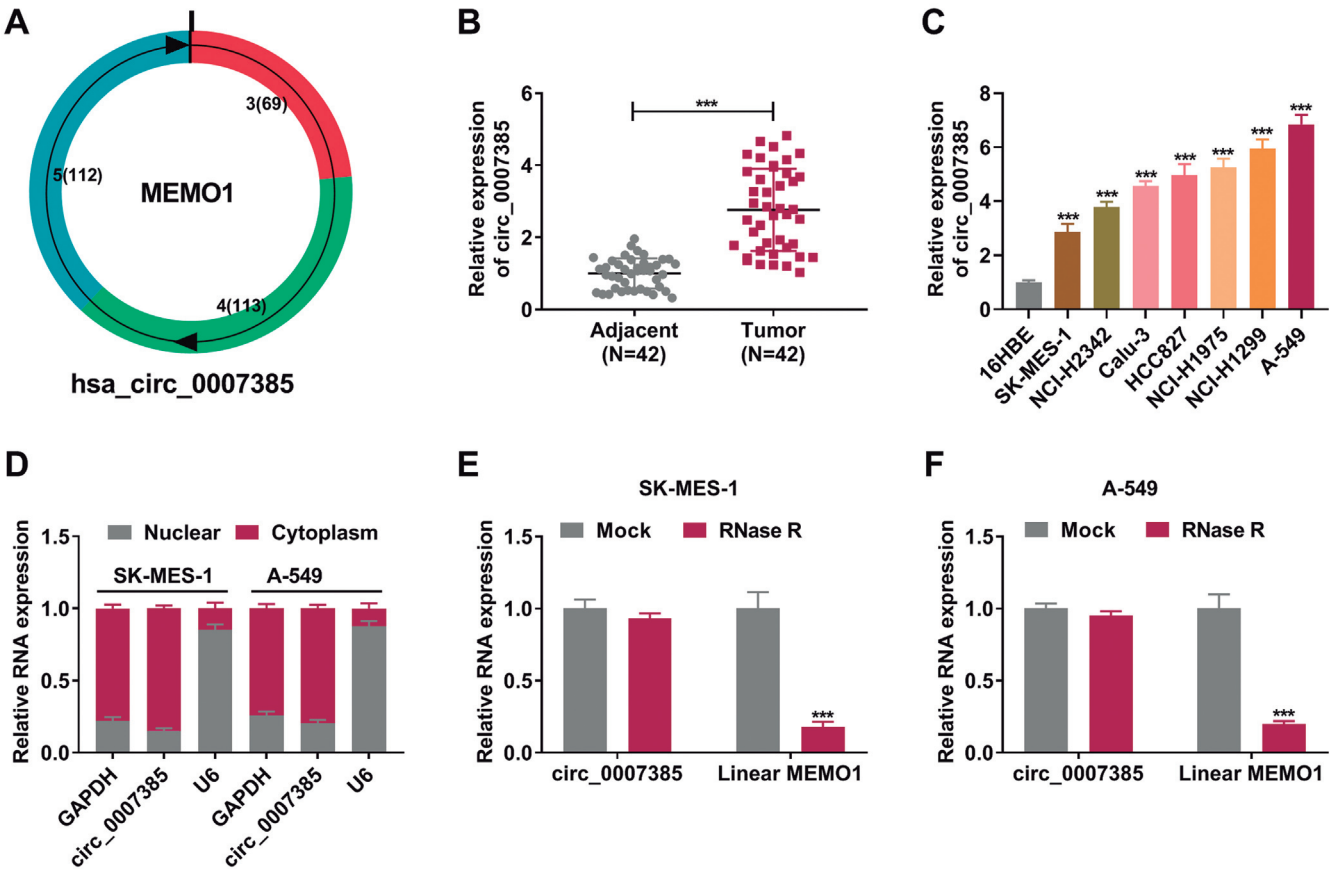

Fig. 1. Circ_0007385 is aberrantly up-regulated in NSCLC. **A.** The structure diagram of circ_0007385 was shown. Circ_0007385 was generated from the cyclization of exon 3, 4 and 5 in MEMO1 gene. **B.** RT-qPCR was adopted to determine the level of circ_0007385 in NSCLC tissue samples (n=42) and adjacent normal tissue samples (n=42). **C.** The level of circ_0007385 was examined in 16HBE and seven NSCLC cell lines by RT-qPCR. **D.** The subcellular localization of circ_0007385 was analyzed with GAPDH and U6 as cytoplasmic marker and nuclear marker. **E, F.** The circular structure of circ_0007385 was tested by exonuclease RNase R with its linear counterpart MEMO1 as the control. ***P<0.001.

apoptotic rate (the percentage of NSCLC cells with $FITC^{+}$ and $PI^{+/-}$) was analyzed.

Western blot assay

Protein samples were acquired via whole cell lysis buffer (Beyotime, Shanghai, China). Protein samples (30 μg) were loaded onto sodium dodecyl sulfate-polyacrylamide gel electrophoresis (SDS-PAGE) and electro-transferred onto polyvinylidene difluoride (PVDF) membrane (Bio-Rad). After sealing with 5% skimmed milk, the membrane was incubated with primary antibodies (Abcam, Cambridge, MA, USA) against B cell leukemia/lymphoma 2 (Bcl-2; Cat. No. ab692), Bcl-2 associated X, apoptosis regulator (Bax; Cat. No. ab243140), LMO3 (Cat. No. ab230490) and GAPDH (Cat. No. ab181603). The primary antibody was then conjugated to the secondary antibody (Abcam). The enhanced chemiluminescence (ECL) reagent (Millipore) and X-ray films (Sangon Biotech) were utilized to expose protein bands.

Prediction of circRNA-miRNA-mRNA axis

Circ_0007385-miRNAs interactions were predicted by three bioinformatics softwares, containing starBase

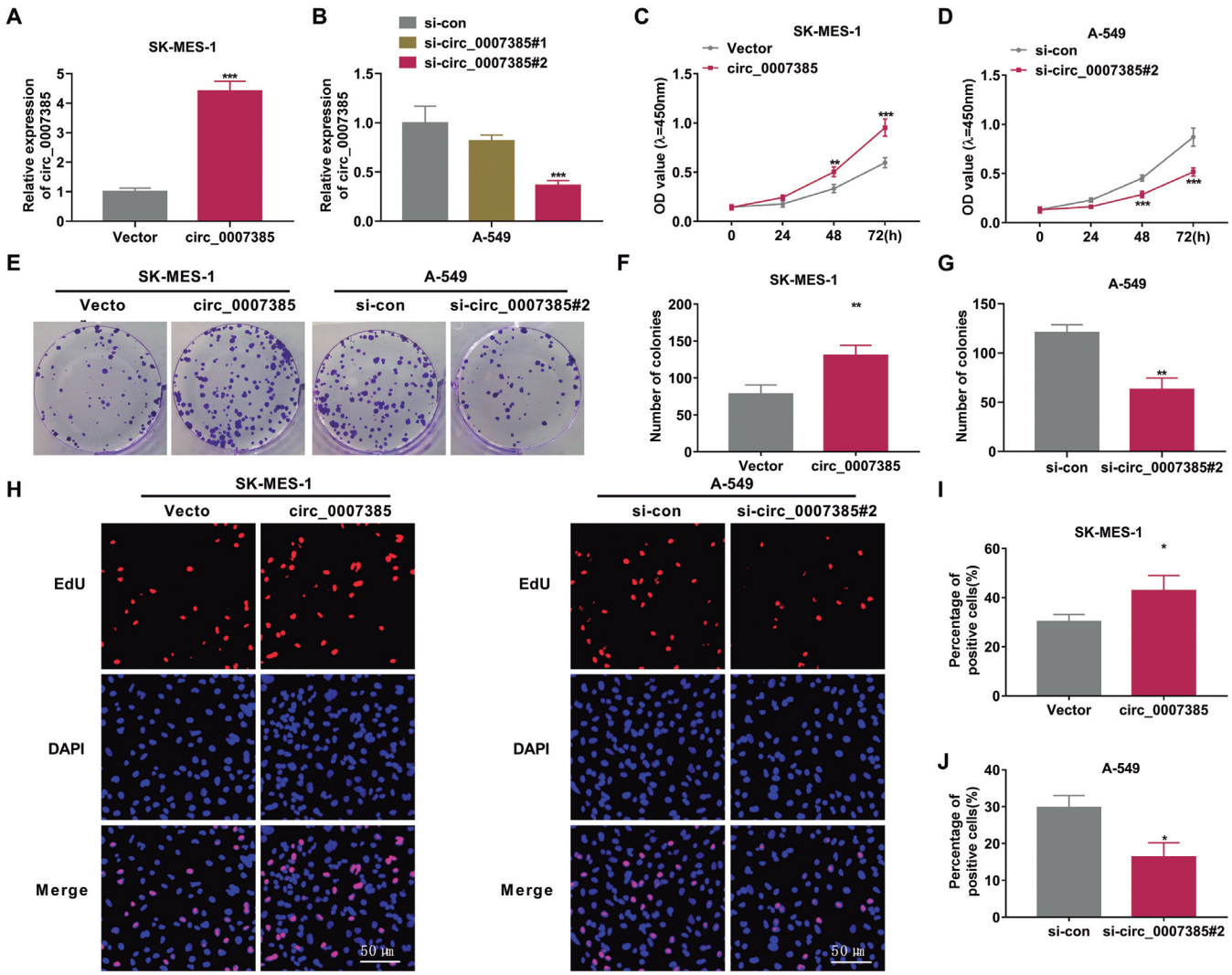

Fig. 2. Circ_0007385 promoted the proliferation of NSCLC cells. **A.** The overexpression efficiency of circ_0007385 plasmid was tested in SK-MES-1 cells by RT-qPCR. **B.** RT-qPCR assay was adopted to analyze the silencing efficiencies of two circ_0007385 siRNAs (si-circ_0007385#1 and si-circ_0007385#2) in A-549 cells. **C-J.** SK-MES-1 cells were transfected with Vector or circ_0007385, whereas A-549 cells were introduced with si-circ_0007385#2 or si-con. **C, D.** The effects of circ_0007385 overexpression and knockdown on cell proliferation were assessed using CCK8 assay. **E-G.** Colony formation assay was applied to analyze cell proliferation through measuring the number of colonies. **H-J.** EdU assay was adopted to evaluate cell proliferation through measuring the incorporation of EdU. *P<0.05, **P<0.01, ***P<0.001.

(http://starbase.sysu.edu.cn), CircInteractome (https://circinteractome.irp.nia.nih.gov) and circBank (http://www.circbank.cn). TargetScan (http://www.targetscan.org) was utilized to predict miR-337-3p-mRNAs interactions.

Dual-luciferase reporter assay

The partial fragments of circ_0007385 and the 3' untranslated region (3'UTR) of LMO3 were constructed into commercial pGL4 plasmid (Promega, Fitchburg, WI, USA) to obtain circ_0007385 WT and LMO3 3'UTR WT. The mutant luciferase reporter plasmids (circ_0007385 MUT and LMO3 3'UTR MUT) were similarly constructed. NSCLC cells in 24-well plates were co-introduced with miR-337-3p/miR-NC (10 μM) and either circ_0007385 WT/MUT (300 ng) or LMO3 3'UTR WT/MUT (300 ng). The relative luciferase intensity was calculated via commercial dual-luciferase reporter system kit (Promega) as Firefly/Renilla.

RNA immunoprecipitation (RIP) assay

Commercial EZ-Magna RIP™ Kit (Millipore) was adopted to perform RIP assay to confirm the intermolecular interactions. Cell lysates were obtained using RIP lysis buffer added with RNase inhibitor (Millipore). Subsequently, RNA samples were mixed with magnetic beads pre-coated with Argonaute2 (Ago2; Abcam) antibody or Immunoglobulin G (IgG; Abcam) antibody. RNA enrichment was examined via RT-qPCR.

Xenograft assay in vivo

Athymic BALB/c nude mice (five mice/group) were acquired from Vital River Laboratory Animal Technology (Beijing, China). A-549 cells, stably transfected with sh-circ_0007385 or sh-con, were inoculated into the mice. Tumor dimension was continuously monitored as length×width^2×0.5. Mice were sacrificed after 28-d inoculation, and tumor weight

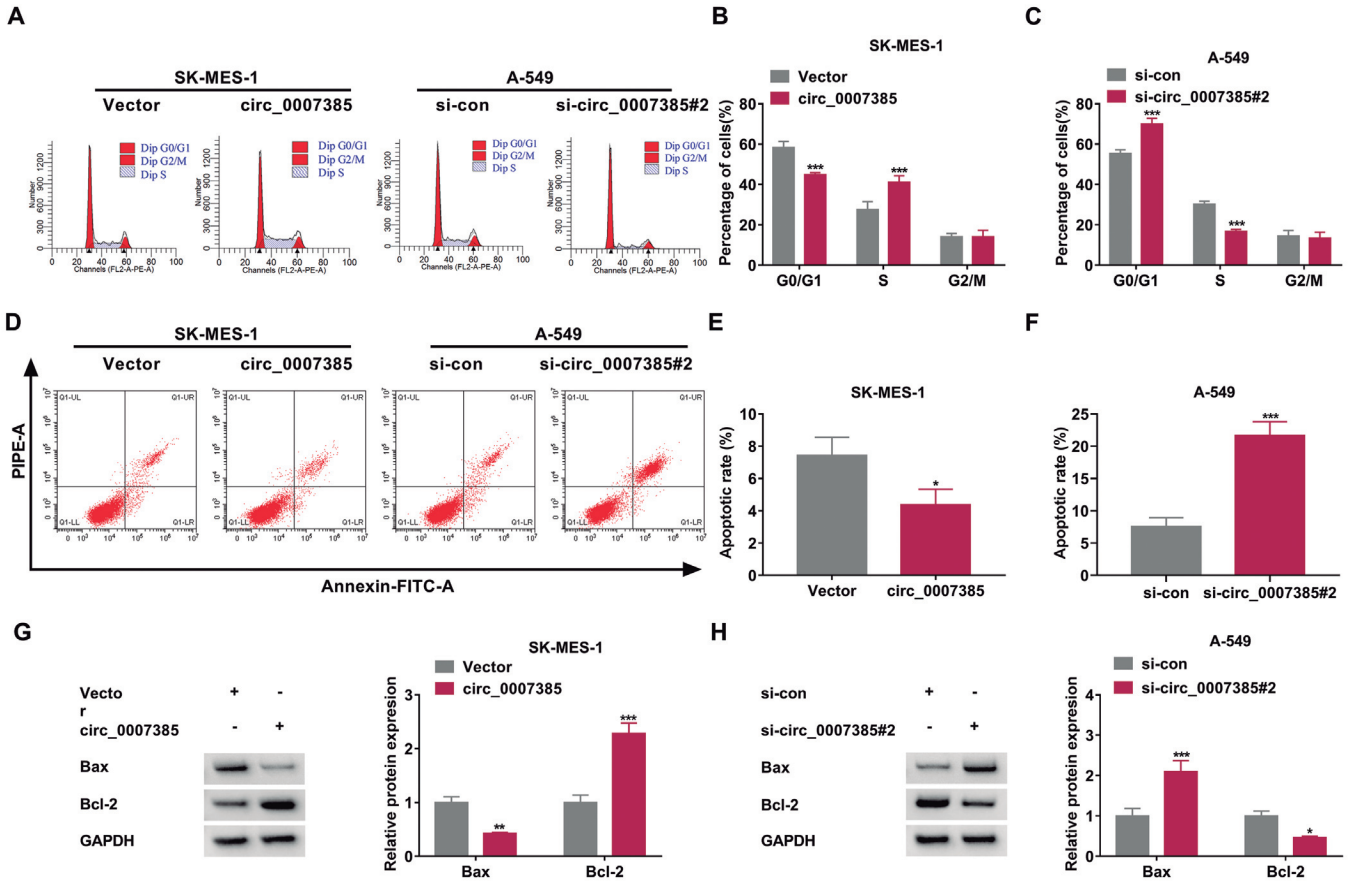

Fig. 3. Circ_0007385 restrained the apoptosis of NSCLC cells. SK-MES-1 cells were transfected with Vector or circ_0007385, whereas A-549 cells were introduced with si-circ_0007385#2 or si-con. **A-C.** Flow cytometry was applied to analyze the proportion of NSCLC cells in different stages of cell cycle progression to assess cell proliferation ability. **D-F.** Cell apoptosis was analyzed by flow cytometry. **G, H.** Western blot assay was conducted to assess cell apoptosis through measuring the level of pro-apoptotic protein (Bax) and anti-apoptotic protein (Bcl-2). *P<0.05, **P<0.01, ***P<0.001.

was recorded. Immunohistochemistry (IHC) assay was adopted using the antibodies against LMO3 (ab230490; 1:300; Abcam) and ki-67 (ab92742; 1:500; Abcam). Protocols in animal assay were approved by the Animal care Committee of Yantai Affiliated Hospital of Binzhou Medical University.

Statistical analysis

Data collected from three independent experiments were analyzed by GraphPad Prism 7.0 software (GraphPad, La Jolla, CA, USA) and the results were represented in the form of mean ± standard deviation

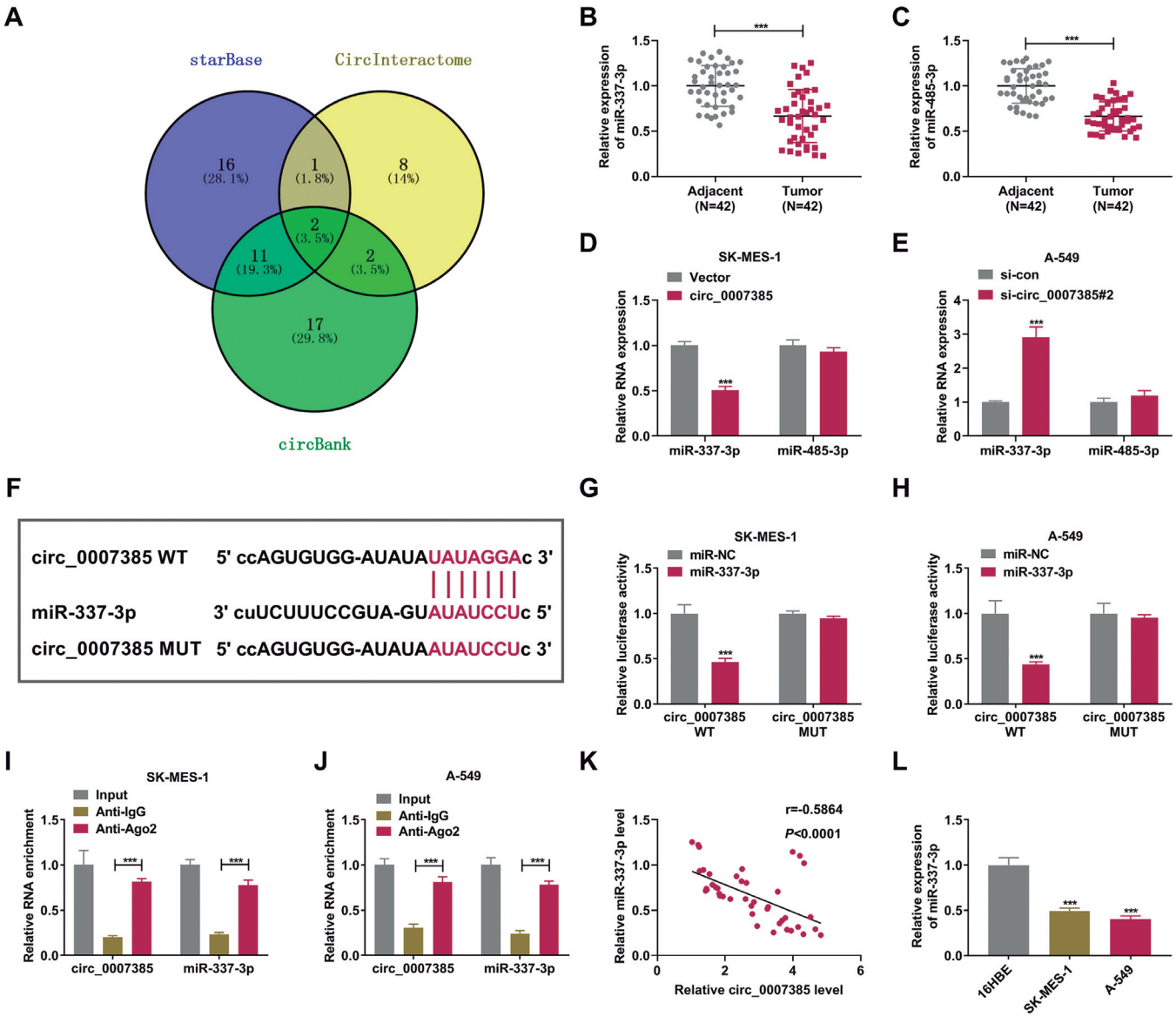

Fig. 4. Circ_0007385 acts as a sponge for miR-337-3p. **A.** Venn diagram showing the candidate targets of circ_0007385 predicted by three bioinformatics databases (starBase, CircInteractome and circBank). Two miRNAs (miR-337-3p and miR-485-3p) were common candidate targets of circ_0007385 predicted by three databases. **B, C.** RT-qPCR was adopted to analyze the expression of miR-337-3p and miR-485-3p in 42 pairs of NSCLC tissue samples and adjacent normal tissue samples. **D.** The levels of miR-337-3p and miR-485-3p were determined in SK-MES-1 cells transfected with Vector or circ_0007385 by RT-qPCR. **E.** The levels of miR-337-3p and miR-485-3p were examined in circ_0007385-silenced A-549 cells by RT-qPCR. **F.** The predicted binding sequence with miR-337-3p in circ_0007385 is shown. **G, H.** Dual-luciferase reporter assay was adopted to verify the target relation between miR-337-3p and circ_0007385. **I, J.** RIP assay was applied to validate the interaction between miR-337-3p and circ_0007385. **K.** The linear correlation between the expression of circ_0007385 and miR-337-3p was analyzed by Spearman's correlation coefficient. **L.** The level of miR-337-3p was determined in 16HBE, SK-MES-1 and A-549 cells by RT-qPCR. ***P<0.001.

(SD). Comparison was estimated via Student's t-test or one-way analysis of variance (ANOVA). Linear relation of expression between molecules was assessed via Spearman's correlation coefficient. The difference was designated as statistically significant with P value of less than 0.05.

Results

Circ_0007385 is aberrantly up-regulated in NSCLC

Circ_0007385 was derived from the back-splicing of exon 3, 4, 5 of MEMO1 gene (Fig. 1A). We analyzed the expression characteristic of circ_0007385 in NSCLC. Circ_0007385 was notably up-regulated in NSCLC tumor tissues when compared with adjacent normal tissues (Fig. 1B). Meanwhile, the correlation between circ_0007385 expression and the pathological parameters of NSCLC patients was assessed. We found that NSCLC patients with high expression of circ_0007385 were significantly associated with advanced TNM stage, large tumor size, positive lymph node metastasis, and poorly differentiated histology grade (Table 2), suggesting that circ_0007385 might be a novel prognostic bio-marker for NSCLC patients. Compared with human bronchial epithelial cell line 16HBE, circ_0007385 was notably up-regulated in all seven NSCLC cell lines (Fig. 1C). Before analyzing the biological function of circ_0007385, we assessed its subcellular distribution and stability. As shown in Figure 1D, circ_0007385 was mainly distributed in the cytoplasmic fraction of NSCLC cells. Linear MEMO1 level was markedly reduced upon exonuclease RNase R digestion, whereas circ_0007385 was resistant to RNase R digestion (Fig. 1E,F), manifesting that circ_0007385 was a circular transcript. There might be some association between abnormal up-regulation of circ_0007385 and NSCLC progression.

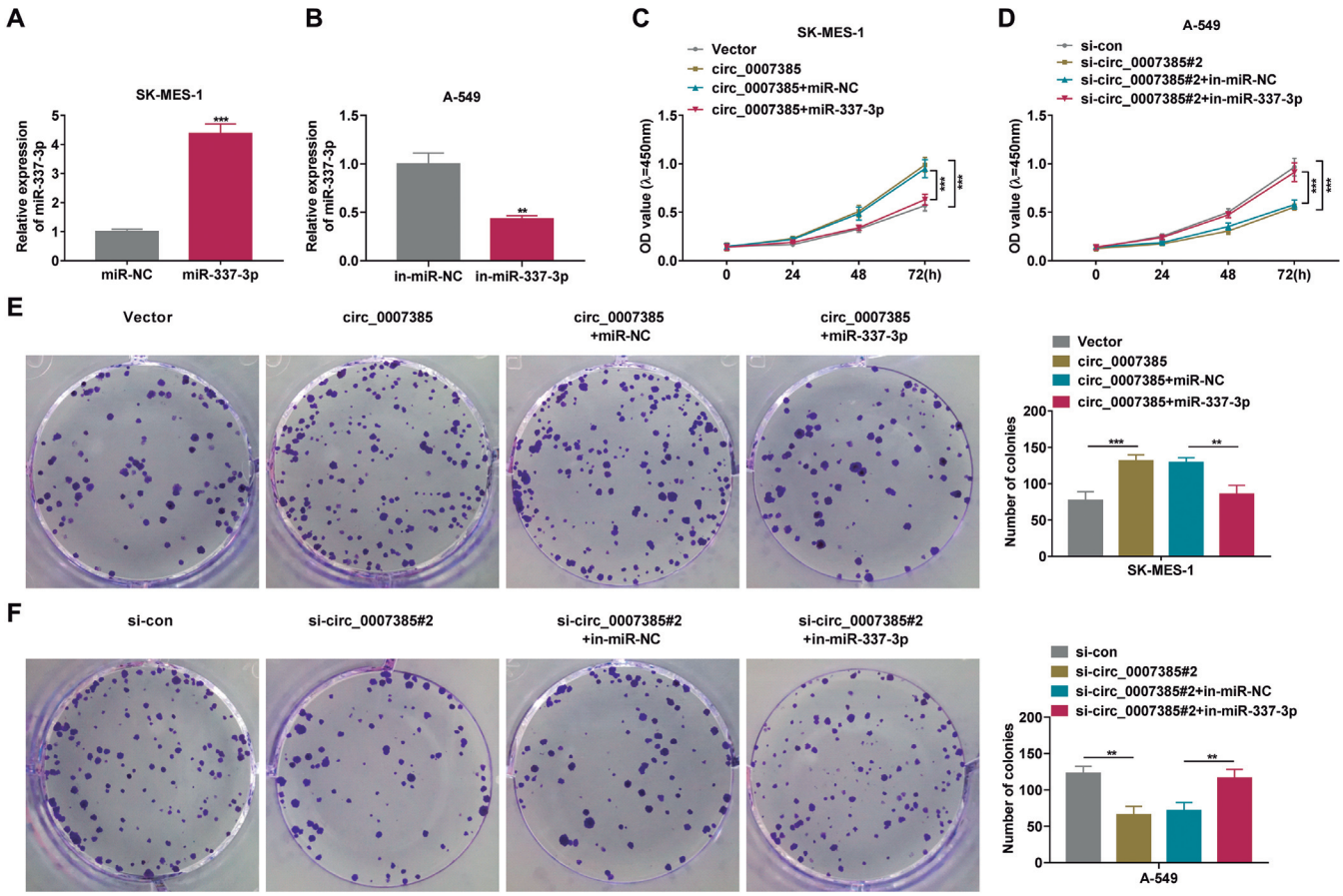

Fig. 5. Circ_0007385 elevates the malignant potential of NSCLC cells partly through sponging miR-337-3p. **A.** The transfection efficiency of miR-337-3p mimics (miR-337-3p) was measured in SK-MES-1 cells by RT-qPCR assay. **B.** The transfection efficiency of miR-337-3p inhibitor (in-miR-337-3p) was determined in A-549 cells by RT-qPCR. (C-N) SK-MES-1 cells were transfected with circ_0007385 alone or together with miR-337-3p, whereas A-549 cells were transfected with si-circ_0007385#2 alone or together with in-miR-337-3p. **C, D.** CCK8 assay was utilized to assess cell proliferation. **E, F.** Colony formation assay was carried out to analyze cell proliferation. **P<0.01, ***P<0.001.

Circ_0007385 acts as an oncogene to promote the proliferation and restrain the apoptosis of NSCLC cells

Gain-of-function and loss-of-function experiments were carried out to analyze the biological functions of circ_0007385 in NSCLC cells. SK-MES-1 cell line was selected for gain-of-function experiments because it has the lowest expression of circ_0007385 among seven NSCLC cell lines, and we chose A-549 for loss-of-function experiments because it had the highest expression of circ_0007385 (Fig. 1C). Overexpression efficiency of circ_0007385 plasmid was high in SK-MES-1 cells (Fig. 2A). Only si-circ_0007385#2 transfection notably reduced circ_0007385 level in A-549 cells, thus it was selected for further analysis (Fig. 2B). Circ_0007385 overexpression promoted the proliferation ability, whereas circ_0007385 knockdown suppressed the proliferation ability of NSCLC cells (Fig. 2C,D). Apart from CCK8 assay, colony formation assay, EdU assay and flow cytometry were applied to further analyze the role of circ_0007385 on cell proliferation. Circ_0007385 overexpression increased the number of colonies, whereas the number of colonies was markedly decreased in circ_0007385-silenced group (Fig. 2E-G). The incorporation of EdU was elevated in circ_0007385-overexpressed cells, whereas circ_0007385 knockdown suppressed the incorporation of EdU (Fig. 2H-J). With the overexpression of circ_0007385, the percentage of NSCLC cells in G0/G1 was reduced and the ratio of cells in S phase was elevated (Fig. 3A,B). On the contrary, circ_0007385 interference elevated the proportion of cells in G0/G1 whereas it reduced the proportion of cells in S phase (Fig. 3A-C). These results demonstrated that circ_0007385 overexpression promoted cell cycle progression of NSCLC cells. Circ_0007385 overexpression reduced the apoptotic rate whereas circ_0007385 knockdown induced the apoptosis of NSCLC cells (Fig. 3D-F). Circ_0007385 overexpression reduced Bax expression and induced Bcl-2

Table 2. The correlation between circ_0007385 expression and the pathological parameters of NSCLC patients (n=42).

Parameter	Relative expression of circ_0007385			
	n	Low (n=21)	High (n=21)	P value
Age (years)				0.7557
<60	18	8	10	
≥60	24	13	11	
Gender				0.5204
Male	27	12	15	
Female	15	9	6	
Smoking				0.1809
Yes	29	17	12	
NO	13	4	9	
TNM stage				0.0016*
I-II	23	17	6	
III-IV	19	4	15	
Tumor size (cm)				0.0036*
T<4	26	18	8	
T≥4	16	3	13	
Lymph node metastasis				0.0109*
No	25	17	8	
Yes	17	4	13	
Histology grade				0.0203*
Poorly and unknown	14	3	11	
Well and moderate	28	18	10	

Fisher's exact test. *P<0.05.

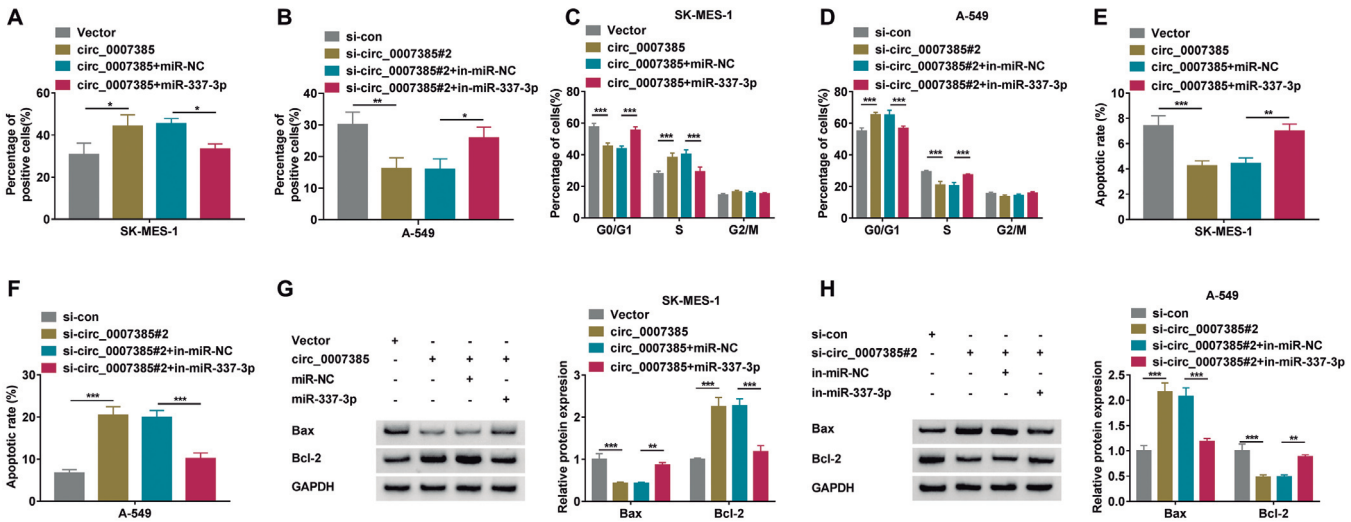

Fig. 6. Circ_0007385 elevates NSCLC cell progression by miR-337-3p. **A, B.** EdU assay was applied to analyze cell proliferation ability. **C, D.** Cell cycle progression was assessed by flow cytometry. **E, F.** The apoptotic rate of NSCLC cells was analyzed by flow cytometry. **G, H.** The protein levels of Bax and Bcl-2 were determined by Western blot assay. *P<0.05, **P<0.01, ***P<0.001.

expression in NSCLC cells, and circ_0007385 interference exhibited an opposite phenomenon (Fig. 3G,H). These results together manifested that circ_0007385 exerted an oncogenic role to promote cell proliferation and inhibit cell apoptosis in NSCLC cells.

Circ_0007385 acts as a sponge for miR-337-3p

The circ_0007385-miRNAs interactions were explored using three bioinformatics databases, including starBase, CircInteractome and circBank. Two miRNAs (miR-337-3p and miR-485-3p) were predicted to be targets of circ_0007385 by all three databases (Fig. 4A). Both the levels of miR-337-3p and miR-485-3p were significantly reduced in NSCLC tissues relative to adjacent normal tissues (Fig. 4B,C). With the overexpression of circ_0007385, miR-337-3p was down-regulated in SK-MES-1 cells (Fig. 4D). In addition, circ_0007385 silencing increased the level of miR-337-3p in A-549 cells (Fig. 4E). The putative binding sites between circ_0007385 and miR-337-3p are shown in Figure 4F. MiR-337-3p overexpression notably reduced the luciferase intensity of luciferase reporter plasmid circ_0007385 WT rather than circ_0007385 MUT (Fig. 4G,H). Circ_0007385 and miR-337-3p were both enriched in Ago2 antibody group (Fig. 4I-J), suggesting their spatial binding in RNA-induced silencing complex (RISC). MiR-337-3p expression exhibited an opposite tendency to circ_0007385 (Fig. 4K). Compared with 16HBE, miR-337-3p expression was notably reduced in both NSCLC cell lines (Fig. 4L). These results together demonstrated that miR-337-3p was a target of circ_0007385, and circ_0007385 negatively modulated miR-337-3p expression in NSCLC cells.

Circ_0007385 elevates the malignant potential of NSCLC cells partly through sponging miR-337-3p

The transfection efficiencies of miR-337-3p mimics (miR-337-3p) and miR-337-3p inhibitor (in-miR-337-3p) were high in NSCLC cells (Fig. 5A,B). Based on the results of CCK8 assay, colony formation assay, EdU assay and flow cytometry, circ_0007385 overexpression-mediated promoting effect on the proliferation ability of NSCLC cells was overturned by the overexpression of miR-337-3p (Figs. 5C-E, 6A-C). Meanwhile,

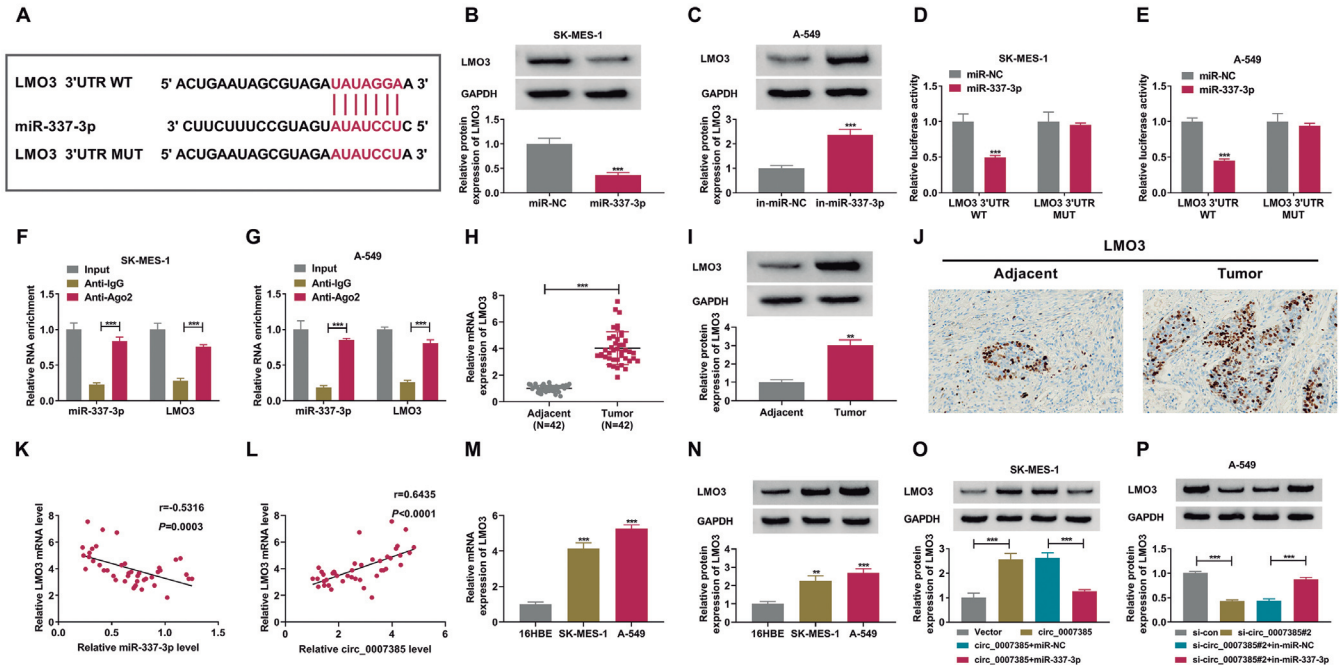

Fig. 7. MiR-337-3p interacts with the 3'UTR of LMO3. **A.** The putative binding sites between miR-337-3p and LMO3 were predicted by TargetScan database. **B.** The effect of miR-337-3p overexpression on the expression of LMO3 in SK-MES-1 cells was analyzed by Western blot assay. **C.** The protein level of LMO3 was determined in NSCLC cells with the silencing of miR-337-3p or not by Western blot assay. **D, E.** The target binding between miR-337-3p and LMO3 was verified using dual-luciferase reporter assay. **F, G.** The intermolecular interaction between miR-337-3p and LMO3 was confirmed using RIP assay. **H, I.** The expression of LMO3 in mRNA and protein levels was examined in NSCLC tissue samples and adjacent normal tissue samples by RT-qPCR and Western blot assay. **J.** IHC assay was employed to analyze the protein level of LMO3 in adjacent normal tissue and NSCLC tissue. **K, L.** Spearman's correlation coefficient was utilized to assess the linear correlation between LMO3 and miR-337-3p or circ_0007385. **M, N.** The mRNA and protein expression of LMO3 was determined in NSCLC cell lines (SK-MES-1 and A-549) and 16HBE cells by RT-qPCR and Western blot assay. **O.** The protein level of LMO3 was determined in SK-MES-1 cells transfected with Vector, circ_0007385, circ_0007385 + miR-NC or circ_0007385 + miR-337-3p by Western blot assay. **P.** Western blot assay was adopted to measure the protein expression of LMO3 in A-549 cells introduced with si-circ_0007385#2 alone or together with in-miR-337-3p. **P<0.01, ***P<0.001.

circ_0007385 knockdown-induced suppressive effect on the proliferation of NSCLC cells was reversed by the interference of miR-337-3p (Fig. 5D,F, 6B-D). Through performing flow cytometry and Western blot assay, we found that miR-337-3p overexpression promoted the apoptosis in circ_0007385-overexpressed NSCLC cells (Fig. 6E-G), and the knockdown of miR-337-3p restrained circ_0007385 silencing-induced apoptosis in NSCLC cells (Fig. 6F-H). These results manifested that circ_0007385 acted as an oncogene to contribute to NSCLC progression partly through absorbing miR-337-3p.

MiR-337-3p interacts with the 3'UTR of LMO3

We predicted the downstream targets of miR-337-3p using bioinformatics database TargetScan, and LMO3 was a possible target of miR-337-3p (Fig. 7A). A negative regulatory relationship between miR-337-3p and LMO3 was found in NSCLC cells (Fig. 7B,C). Luciferase activity was markedly reduced in wild type reporter plasmid (LMO3 3'UTR WT) with the accumulation of miR-337-3p, and the overexpression of miR-337-3p had no effect on the luciferase activity of mutant reporter plasmid (LMO3 3'UTR MUT) (Fig. 7D,E), suggesting the target relation between miR-337-3p and LMO3. Furthermore, the target relation between miR-337-3p and LMO3 was also verified by RIP assay (Fig. 7F,G). LMO3 mRNA and protein expression were both up-regulated in NSCLC tumor tissues relative to that in adjacent normal tissues (Fig. 7H,I). High protein level of LMO3 in NSCLC tissue compared with adjacent normal tissue was also confirmed by IHC assay (Fig. 7J). MiR-337-3p expression was negatively correlated

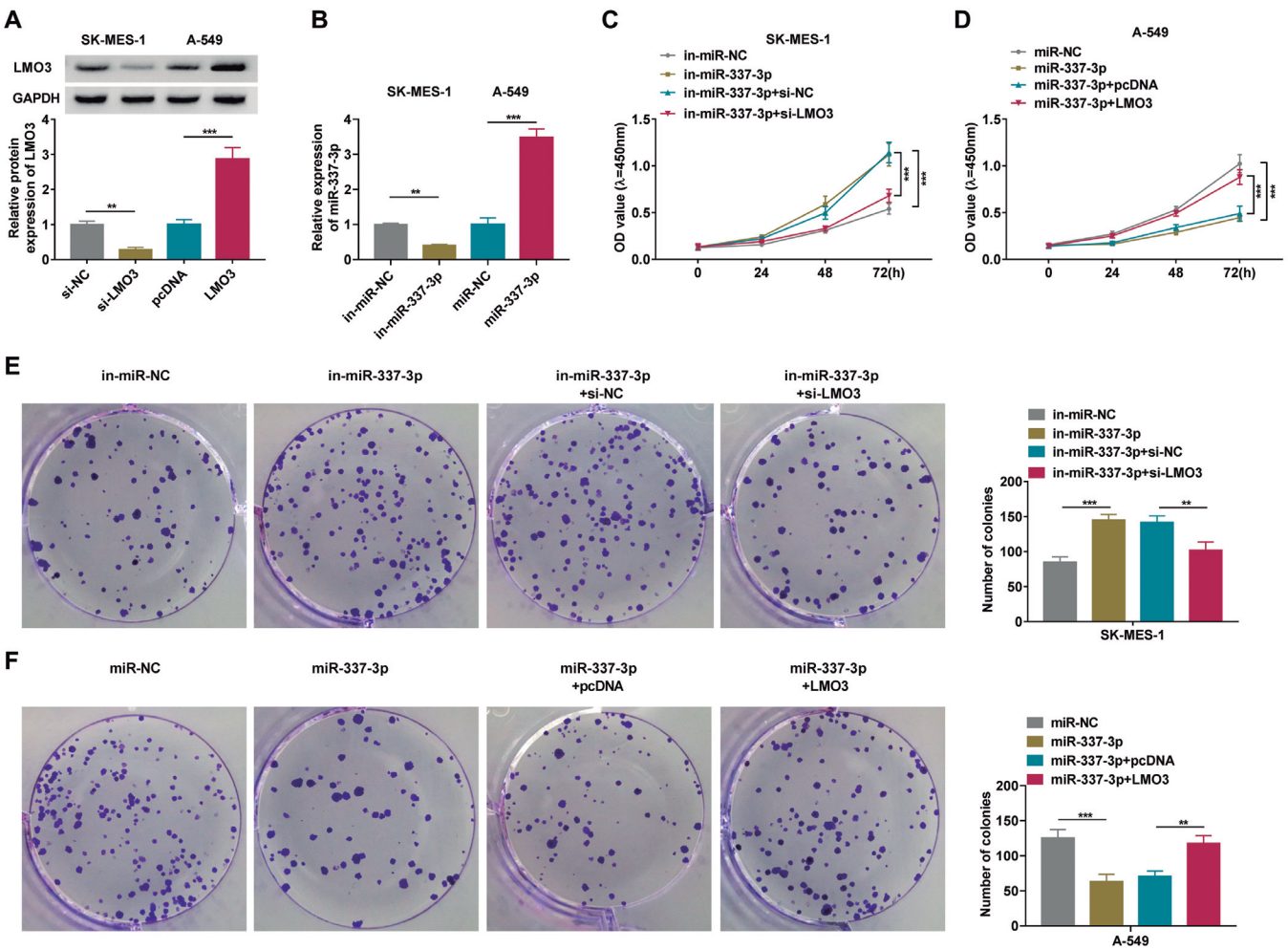

Fig. 8. MiR-337-3p overexpression restrains the malignant potential of NSCLC cells partly through down-regulating LMO3. **A.** The silencing and overexpression efficiencies of si-LMO3 and LMO3 plasmid were determined in NSCLC cells by Western blot assay. **B.** RT-qPCR was adopted to assess the transfection efficiencies of in-miR-337-3p and miR-337-3p in NSCLC cells. (C-N) SK-MES-1 cells were transfected with in-miR-337-3p alone or together with si-LMO3, whereas A-549 cells were transfected with miR-337-3p alone or together with LMO3 plasmid. **C, D.** Cell proliferation ability was analyzed by CCK8 assay. **E, F.** The number of colonies was measured by colony formation assay. **P<0.01, ***P<0.001.

with the mRNA level of LMO3 (Fig. 7K), and there was a positive correlation between the expression of LMO3 mRNA and circ_0007385 (Fig. 7L). Compared with 16HBE cell line, both the mRNA and protein levels of LMO3 were up-regulated in NSCLC cell lines (Fig. 7M,N). Circ_0007385 overexpression increased LMO3 protein expression, and the addition of miR-337-3p mimics reduced its protein level again (Fig. 7O). Circ_0007385 knockdown decreased LMO3 expression, and its level was rescued with the introduction of in-miR-337-3p in NSCLC cells (Fig. 7P). Overall, LMO3 was a molecular target of miR-337-3p, and LMO3 was regulated by circ_0007385/miR-337-3p axis in NSCLC cells.

MiR-337-3p overexpression restrains the malignant potential of NSCLC cells partly through down-regulating LMO3

The transfection efficiencies of si-LMO3, LMO3 plasmid, in-miR-337-3p and miR-337-3p were high in NSCLC cells (Fig. 8A,B). The silencing of miR-337-3p promoted the proliferation of NSCLC cells, and the interference of LMO3 reversed miR-337-3p silencing-induced effect on cell proliferation of NSCLC cells (Fig, 8C,E, 9A,C). MiR-337-3p overexpression restrained cell proliferation, and cell proliferation was largely rescued in miR-337-3p and LMO3 co-transfected group (Figure 8D, 8F, 9B and 9D). These results manifested that miR-337-3p suppressed cell proliferation partly through down-regulating LMO3. According to the results of flow cytometry and Western blot assay, we found that miR-337-3p silencing suppressed cell apoptosis, which was overturned by the silencing of LMO3 (Fig. 9E,G). MiR-337-3p accumulation induced the apoptosis of NSCLC cells, and this effect was reversed by the overexpression of LMO3 (Fig. 9F,H). These results demonstrated that LMO3 was indeed a functional target of miR-337-3p in NSCLC cells.

Circ_0007385 knockdown restrains NSCLC progression in vivo

Given the oncogenic role of circ_0007385 *in vitro*, we then analyzed the in vivo role of circ_0007385 on the growth of xenograft tumors. Circ_0007385 silencing markedly suppressed the growth of xenograft tumors (Fig. 10A,B), suggesting that circ_0007385 exerted an oncogenic role in tumor growth *in vivo*. The expression of circ_0007385 and LMO3 mRNA and protein were all reduced in circ_0007385-silenced tumor tissues, whereas miR-337-3p level was enhanced in tumor tissues in sh-circ_0007385 group (Fig. 10C-F). We also assessed the levels of LMO3 and proliferation marker ki-67 in tumor tissues using IHC assay. The silencing of circ_0007385 in tumor tissues caused a marked reduction in the expression of LMO3 and ki-67 (Fig. 10G-H). Western blot assay manifested that circ_0007385 knockdown up-regulated the expression of pro-apoptotic protein (Bax) and reduced the expression of anti-apoptotic protein (Bcl-2) in tumor tissues (Fig. 10I). Taken together, circ_0007385 knockdown blocked xenograft tumor growth *in vivo*.

Discussion

With the development of sequencing technologies and bioinformatics prediction, increasing numbers of

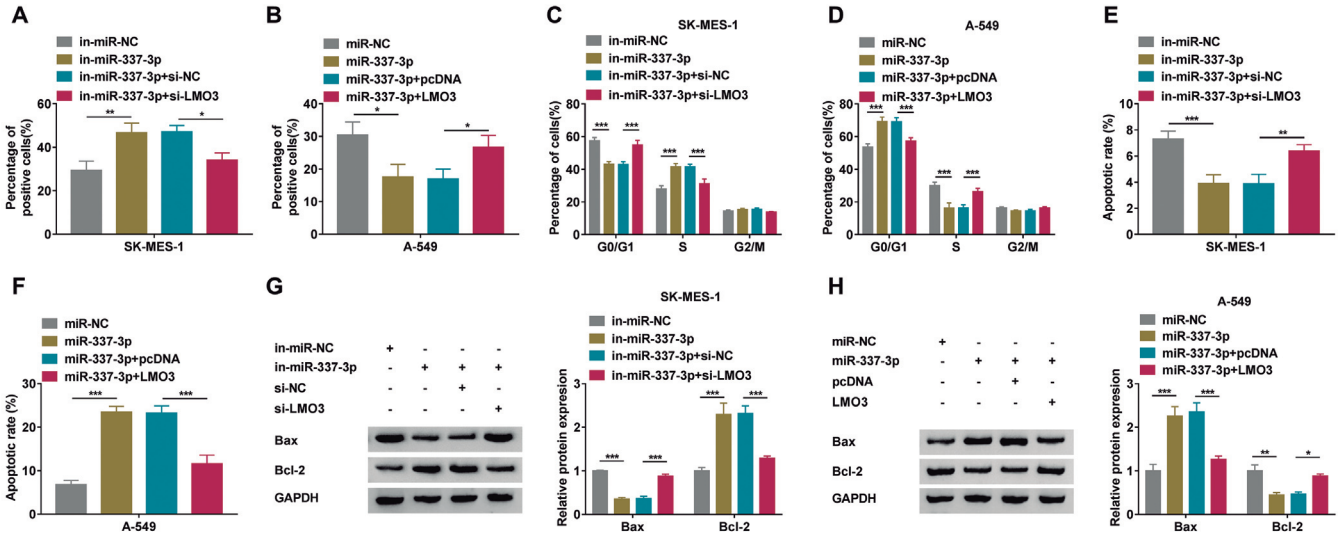

Fig. 9. MiR-337-3p overexpression restrains NSCLC cell progression by LMO3. **A, B.** Cell proliferation ability was assessed by EdU assay. **C, D.** Cell cycle progression was evaluated by flow cytometry. **E, F.** The apoptosis of NSCLC cells was measured by flow cytometry. **G, H.** The protein levels of Bax and Bcl-2 were determined by Western blot assay. *P<0.05, **P<0.01, ***P<0.001.

circRNAs have been discovered and defined (Wang et al., 2019; Sun et al., 2020). CircRNAs are a class of novel non-coding RNAs closely related to cancer initiation, progression and metastasis (Yang et al., 2017). We intended to analyze the biological functions of circ_0007385 in NSCLC and explore its working mechanism.

Circ_0007385 exerted a carcinogenic role in NSCLC progression. For instance, Jiang et al. demonstrated that circ_0007385 was aberrantly up-regulated in NSCLC, and circ_0007385 silencing restrained malignant phenotypes in NSCLC cells (Jiang et al., 2018). Ye et al. found that circ_0007385 knockdown hampered the proliferation, motility and cisplatin resistance of NSCLC cells via mediating the miR-519d-3p/HMGB1 axis (Ye et al., 2020). Lin et al. reported that circ_0007385 expression was enhanced in NSCLC tumor tissues, and a high level of circ_0007385 was correlated with dismal prognosis in NSCLC patients (Lin et al., 2020). These studies all confirmed the carcinogenic role of circ_0007385 in NSCLC. Consistent with these studies, we found that circ_0007385 was markedly up-regulated in NSCLC tissues and cell lines, and circ_0007385 accelerated proliferation capacity and hampered apoptosis in NSCLC cells.

More and more studies on circRNAs indicated that circRNAs regulated cell behaviors via functioning as miRNA sponges (Hansen et al., 2013; Panda, 2018). For instance, circ_0001649 restrained NSCLC development by sponging miR-331-3p and miR-338-5p (Liu et al.,

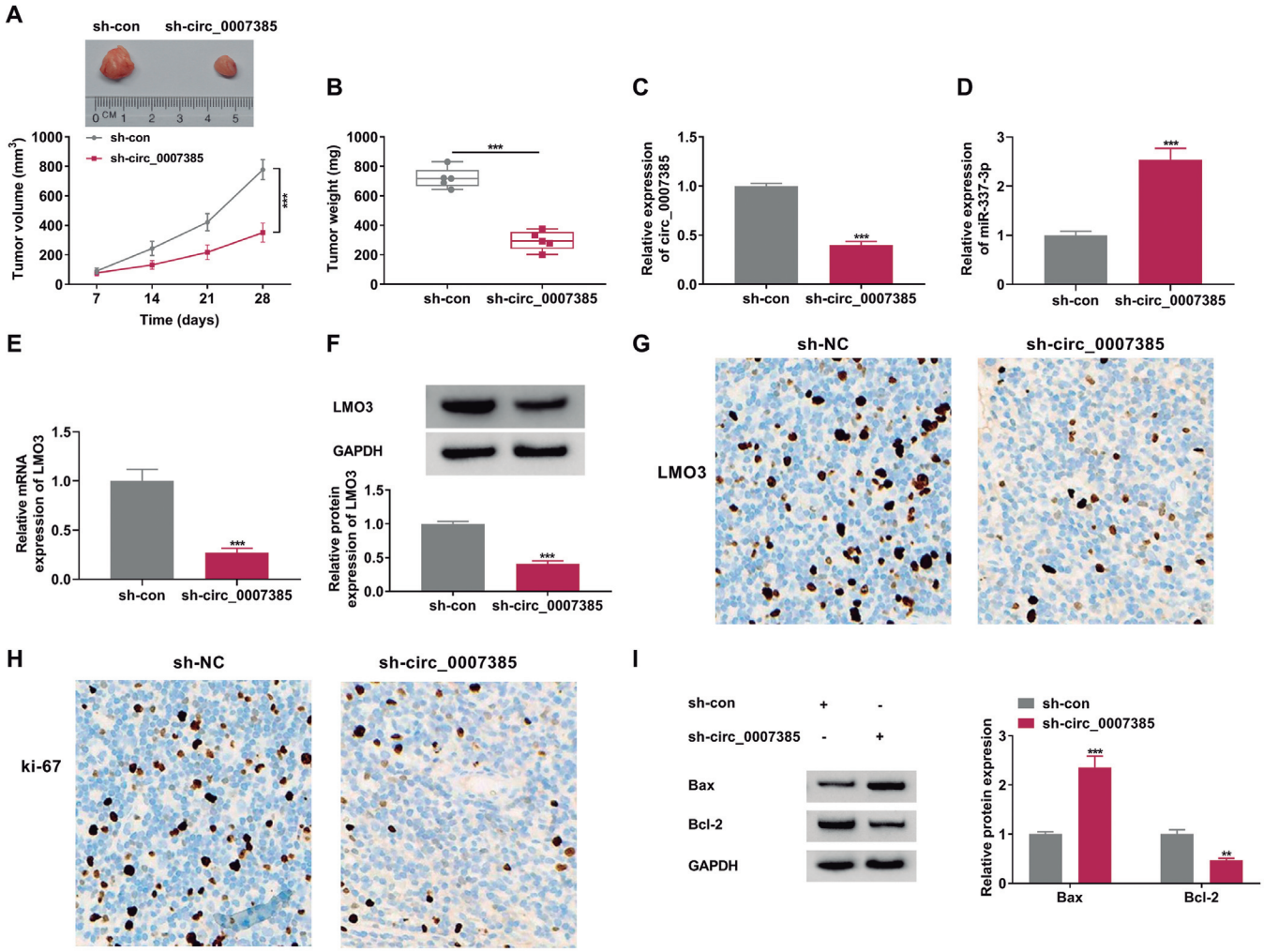

Fig. 10. Circ_0007385 knockdown restrains NSCLC progression in vivo. **A.** Tumor growth curve was drawn through monitoring tumor volume every week using the equation of volume = length×width2×0.5. **B.** Tumor weight was recorded after 28-d injection. **C, D.** The expression of circ_0007385 and miR-337-3p was determined in dissected tumor tissues by RT-qPCR. **E, F.** RT-qPCR and Western blot assay were adopted to detect the mRNA and protein levels of LMO3 in dissected tumor tissues. **G, H.** IHC assay was conducted to measure the levels of LMO3 and proliferation marker (ki-67) in dissected tumor tissues. **I.** The levels of Bax and Bcl-2 were measured in dissected tumor tissues by Western blot assay. **P<0.01, ***P<0.001.

2018). Circ_0018818 suppressed the malignant phenotypes in NSCLC cells through abolishing miR-767-3p (Xu et al., 2020). To better deep understand the carcinogenic mechanism of circ_0007385 in NSCLC, bioinformatics databases starBase, CircInteractome and circBank were utilized to predict the possible miRNA targets of circ_0007385 based on the complementary sites. After screening and verification, the binding of miR-337-3p and circ_0007385 was validated. MiR-337-3p abundance was declined in NSCLC, and it was negatively regulated by circ_0007385 in NSCLC cells. MiR-337-3p exhibited an anti-tumor activity in many malignancies (Du et al., 2012; Li et al., 2019; Wang et al., 2020; Zhang et al., 2020; Meng et al., 2021). In NSCLC, Li et al. found that circ_ZNF124 aggravated NSCLC progression through absorbing miR-337-3p to activate JAK2/STAT3 signaling (Li et al., 2019). MiR-337-3p overexpression enhanced paclitaxel and docetaxel sensitivity in NSCLC cells (Du et al., 2012). MiR-337-3p hampered cell proliferation capacity and accelerated cell apoptosis, and anti-neoplastic function of miR-337-3p was in line with former articles (Du et al., 2012; Li et al., 2019). In addition, we found that circ_0007385 overexpression-mediated effects in NSCLC cells were overturned by the overexpression of miR-337-3p. Meanwhile, circ_0007385 silencing-induced influences were reversed by the knockdown of miR-337-3p in NSCLC cells, suggesting that circ_0007385 exerted a carcinogenic role through suppressing miR-337-3p in NSCLC cells.

Through targeting oncogenes or tumor suppressors, dysregulated miRNAs accelerate or restrain tumor initiation and progression (Fabian et al., 2010; Di Leva et al., 2014). Bioinformatic database TargetScan was utilized to seek possible mRNA targets of miR-337-3p. LMO3 was verified as a target of miR-337-3p in NSCLC cells. LMO3 was a well-characterized oncogenic factor, and it was reported to be related to various cancers, containing NSCLC (Aoyama et al., 2005; Song et al., 2015). Multiple miRNAs exerted their tumor suppressor roles through negatively regulating LMO3 expression (Liu et al., 2015; Xuan et al., 2019). MiR-337-3p reversely modulated LMO3 expression, and LMO3 was highly expressed in NSCLC. LMO3 silencing overturned miR-337-3p knockdown-mediated effects in NSCLC cells. Meanwhile, LMO3 overexpression also reversed miR-337-3p overexpression-induced effects in NSCLC cells, suggesting that miR-337-3p exerted its tumor suppressor role through targeting LMO3 in NSCLC cells. Circ_0007385 indirectly up-regulated LMO3 level via sponging miR-337-3p in NSCLC cells. Using *in vivo* approaches, we found that circ_0007385 knockdown markedly restrained xenograft tumor growth.

Conclusion

In summary, this study found that circ_0007385 was highly expressed in NSCLC tissues and cell lines, and circ_0007385 silencing suppressed the proliferation and induced the apoptosis of NSCLC cells. Furthermore, the miR-337-3p/LMO3 axis was a downstream signaling axis of circ_0007385, and circ_0007385 functioned via targeting the miR-337-3p/LMO3 axis (Fig. 11). These results might improve our understanding of the molecular mechanism behind NSCLC progression.

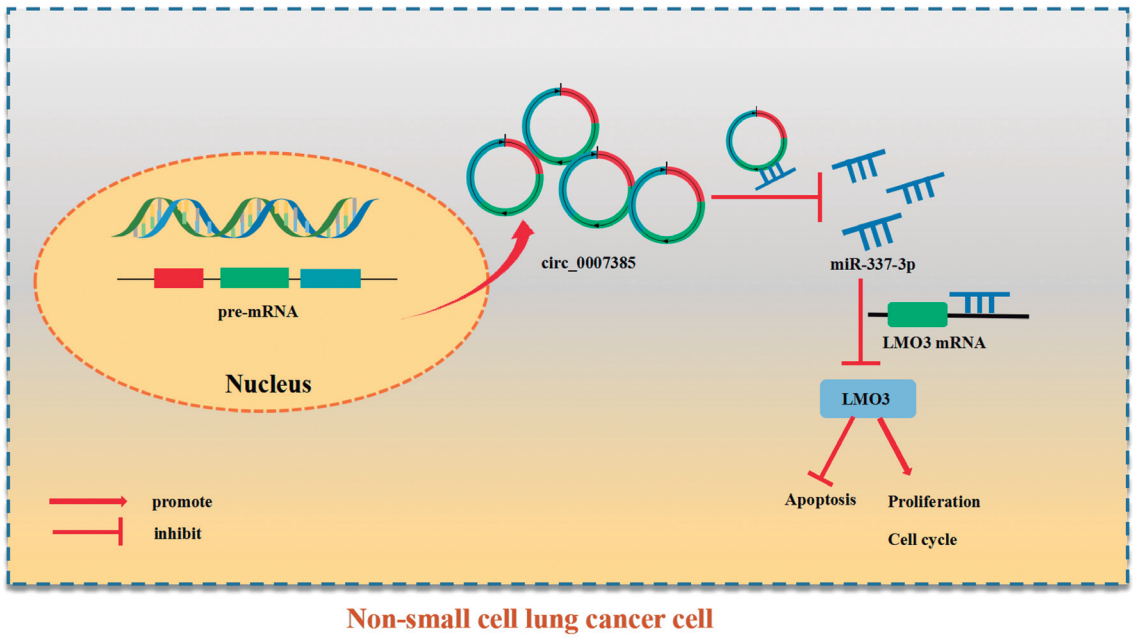

Fig. 11. The mechanism diagram of this study. Circ_0007385 contributes to NSCLC progression by up-regulating LMO3 via sponging miR-337-3p.

Acknowledgements. None.

Disclosure of interest. The authors declare that they have no conflicts of interest.

Funding. None.

Clinical study statement. The research was carried out in accordance with the World Medical Association Declaration of Helsinki, and that all subjects had provided written informed consent.

Availability of data. Not applicable.

References

Aoyama M., Ozaki T., Inuzuka H., Tomotsune D., Hirato J., Okamoto Y., Tokita H., Ohira M. and Nakagawara A. (2005). LMO3 interacts with neuronal transcription factor, HEN2, and acts as an oncogene in neuroblastoma. Cancer Res. 65, 4587-4597.

Chen D., Zhang Y., Lin Y., Shen F., Zhang Z. and Zhou J. (2019). MicroRNA-382 inhibits cancer cell growth and metastasis in NSCLC via targeting LMO3. Exp. Ther. Med. 17, 2417-2424.

Dawid I.B., Breen J.J. and Toyama R. (1998). LIM domains: multiple roles as adapters and functional modifiers in protein interactions. Trends Genet. 14, 156-162.

Di Leva G., Garofalo M. and Croce C.M. (2014). MicroRNAs in cancer. Annu. Rev. Pathol. 9, 287-314.

Du L., Subauste M.C., DeSevo C., Zhao Z., Baker M., Borkowski R., Schageman J.J., Greer R., Yang C.R., Suraokar M., Wistuba I.I., Gazdar A.F., Minna J.D. and Pertsemlidis A. (2012). miR-337-3p and its targets STAT3 and RAP1A modulate taxane sensitivity in non-small cell lung cancers. PLoS One 7, e39167.

Fabian M.R., Sonenberg N. and Filipowicz W. (2010). Regulation of mRNA translation and stability by microRNAs. Annu. Rev. Biochem. 79, 351-379.

Greene J., Baird A.M., Brady L., Lim M., Gray S.G., McDermott R. and Finn S.P. (2017). Circular RNAs: Biogenesis, function and role in human diseases. Front. Mol. Biosci. 4, 38.

Hansen T.B., Jensen T.I., Clausen B.H., Bramsen J.B., Finsen B., Damgaard C.K. and Kjems J. (2013). Natural RNA circles function as efficient microRNA sponges. Nature 495, 384-388.

Jiang M.M., Mai Z.T., Wan S.Z., Chi Y.M., Zhang X., Sun B.H. and Di Q.G. (2018). Microarray profiles reveal that circular RNA hsa_circ_0007385 functions as an oncogene in non-small cell lung cancer tumorigenesis. J. Cancer Res. Clin. Oncol. 144, 667-674.

Li Q., Huang Q., Cheng S., Wu S., Sang H. and Hou J. (2019). Circ_ZNF124 promotes non-small cell lung cancer progression by abolishing miR-337-3p mediated downregulation of JAK2/STAT3 signaling pathway. Cancer Cell Int. 19, 291.

Lin Y., Su W. and Lan G. (2020). Value of circular RNA 0007385 in disease monitoring and prognosis estimation in non-small-cell lung cancer patients. J. Clin. Lab. Anal. 34, e23338.

Liu R., Deng P., Zhang Y., Wang Y. and Peng C (2021). Circ_0082182 promotes oncogenesis and metastasis of colorectal cancer in vitro and in vivo by sponging miR-411 and miR-1205 to activate the Wnt/β-catenin pathway. World J. Surg. Oncol. 19, 51.

Liu X., Lei Q., Yu Z., Xu G., Tang H., Wang W., Wang Z., Li G. and Wu M. (2015). MiR-101 reverses the hypomethylation of the LMO3 promoter in glioma cells. Oncotarget 6, 7930-7943.

Liu T., Song Z. and Gai Y. (2018). Circular RNA circ_0001649 acts as a prognostic biomarker and inhibits NSCLC progression via sponging miR-331-3p and miR-338-5p. Biochem. Biophys. Res. Commun. 503, 1503-1509.

Livak K.J. and Schmittgen T.D. (2001). Analysis of relative gene expression data using real-time quantitative PCR and the 2(-Delta Delta C(T)) Method. Methods 25, 402-408.

Meng Q.H., Li Y., Kong C., Gao X.M. and Jiang X.J. (2021). Circ_0000388 exerts oncogenic function in cervical cancer cells by regulating miR-337-3p/TCF12 axis. Cancer Biother. Radiopharm. 36, 58-69.

Molina J.R., Yang P., Cassivi S.D., Schild S.E. and Adjei A.A. (2008). Non-small cell lung cancer: epidemiology, risk factors, treatment, and survivorship. Mayo Clin. Proc. 83, 584-594.

Panda A.C. (2018). Circular RNAs act as miRNA sponges. Adv. Exp. Med. Biol. 1087, 67-79.

Song Y.F., Hong J.F., Liu D.L., Lin Q.A., Lan X.P. and Lai G.X. (2015). miR-630 targets LMO3 to regulate cell growth and metastasis in lung cancer. Am. J. Transl. Res. 7, 1271-1279.

Sun Q., Li X., Xu M., Zhang L., Zuo H., Xin Y., Zhang L. and Gong P. (2020). Differential expression and bioinformatics analysis of circRNA in non-small cell lung cancer. Front. Genet. 11, 586814.

Toloza E.M., Harpole L., Detterbeck F. and McCrory D.C. (2003). Invasive staging of non-small cell lung cancer: A review of the current evidence. Chest. 123 (1 Suppl), 157s-166s.

Wang C., Tan S., Liu W.R., Lei Q., Qiao W., Wu Y., Liu X., Cheng W., Wei Y.Q., Peng Y. and Li W. (2019). RNA-Seq profiling of circular RNA in human lung adenocarcinoma and squamous cell carcinoma. Mol. Cancer 18, 134.

Wang Z., Yao L., Li Y., Hao B., Wang M., Wang J., Gu W., Zhan H., Liu G. and Wu Q. (2020). miR-337-3p inhibits gastric tumor metastasis by targeting ARHGAP10. Mol. Med. Rep. 21, 705-719.

Xu X., Zhou X., Gao C. and Cui Y. (2020). Hsa_circ_0018818 knockdown suppresses tumorigenesis in non-small cell lung cancer by sponging miR-767-3p. Aging (Albany NY). 12, 7774-7785.

Xuan Y.W., Liao M., Zhai W.L., Peng L.J. and Tang Y. (2019). MicroRNA-381 inhibits lung adenocarcinoma cell biological progression by directly targeting LMO3 through regulation of the PI3K/Akt signaling pathway and epithelial-to-mesenchymal transition. Eur. Rev. Med. Pharmacol. Sci. 23, 8411-8421.

Yang Z., Xie L., Han L., Qu X., Yang Y., Zhang Y., He Z., Wang Y. and Li J. (2017). Circular RNAs: Regulators of cancer-related signaling pathways and potential diagnostic biomarkers for human cancers. Theranostics 7, 3106-3117.

Ye Y., Zhao L., Li Q., Xi C., Li Y. and Li Z. (2020). circ_0007385 served as competing endogenous RNA for miR-519d-3p to suppress malignant behaviors and cisplatin resistance of non-small cell lung cancer cells. Thorac. Cancer 11, 2196-2208.

Zhang Z., Zhang L., Wang B., Wei R., Wang Y., Wan J., Zhang C., Zhao L., Zhu X., Zhang Y., Chu C., Guo Q., Yin X. and Li X. (2020). MiR-337-3p suppresses proliferation of epithelial ovarian cancer by targeting PIK3CA and PIK3CB. Cancer Lett. 469, 54-67.

Accepted November 25, 2022